Electronic Supplementary Information

The effect of the trans axial ligand of cobalt corroles on water oxidation activity in neutral aqueous solutions

Liang Xu,‡[a] Haitao Lei,‡[a] Zongyao Zhang,[a] Zhen Yao,[c] Jianfeng Li,[c] Zhiyong Yu,[a] and Rui Cao*[ab]

[a]Department of Chemistry, Renmin University of China, Beijing 100872, China.

[b]School of Chemistry and Chemical Engineering, Shaanxi Normal University, Xi'an 710119, China.

[c]College of Materials Science and Opto-electronic Technology, University of Chinese Academy of Sciences, Beijing 101408, China.

‡These authors contributed equally to this work.

*Correspondence E-mail: ruicao@ruc.edu.cn

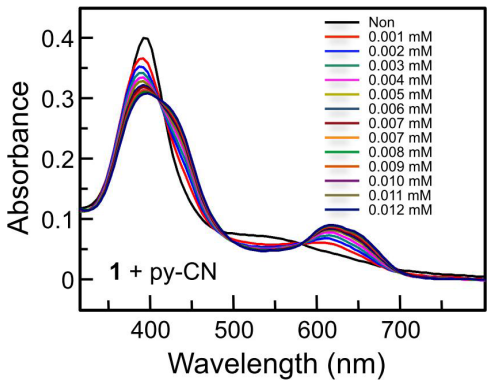

Figure S1. UV-vis spectra of 5 μM **1** in dichloromethane with addition of various amounts of 4-cyanopyridine at room temperature.

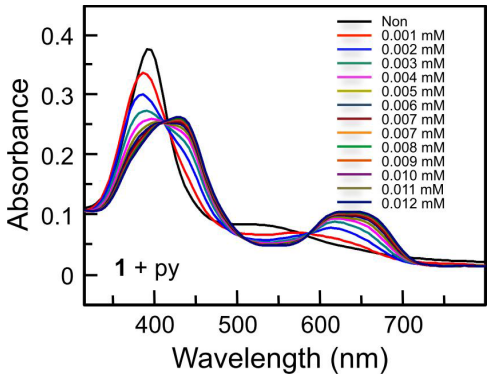

Figure S2. UV-vis spectra of 5 μM **1** in dichloromethane with addition of various amounts of pyridine at room temperature.

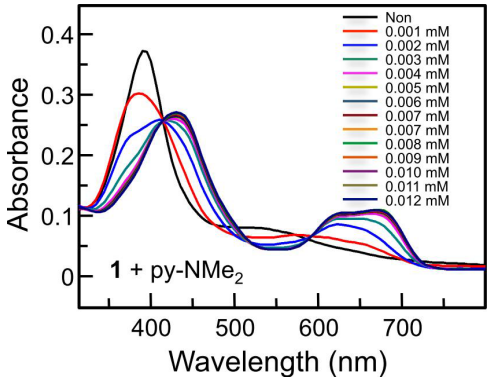

Figure S3. UV-vis spectra of 5 μM **1** in dichloromethane with addition of various amounts of 4-(dimethylamino)pyridine at room temperature.

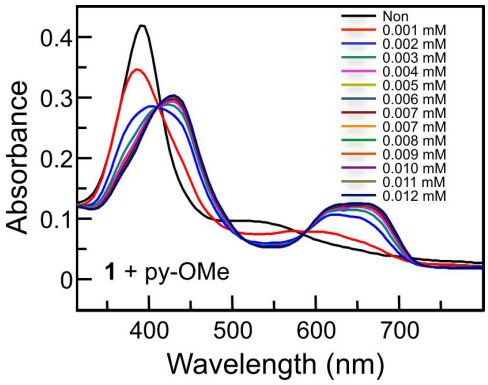

Figure S4. UV-vis spectra of 5 μM **1** in dichloromethane with addition of various amounts of 4-methoxypyridine at room temperature.

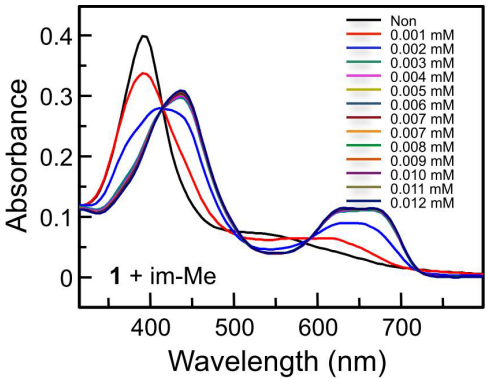

Figure S5. UV-vis spectra of 5 μM **1** in dichloromethane with addition of various amounts of *N*-methylimidazole at room temperature.

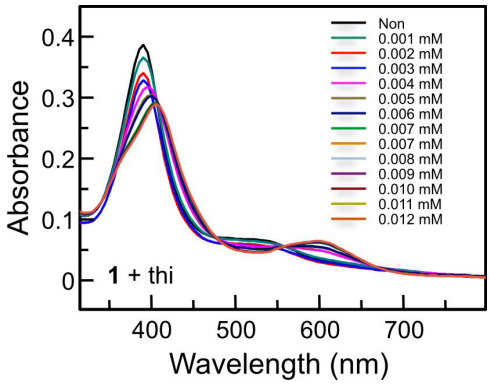

Figure S6. UV-vis spectra of 5 μM **1** in dichloromethane with addition of various amounts of sodium thiophenolate dissolved in methanol at room temperature.

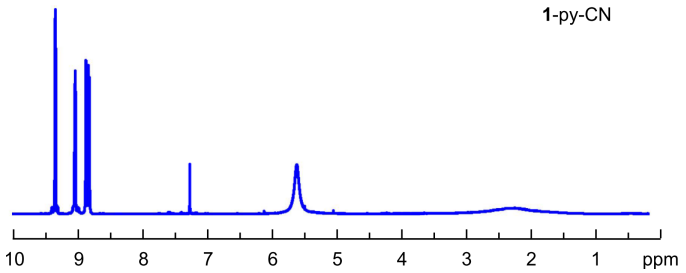

Figure S7. ^{1}H NMR spectrum of **1**-py-CN in $CDCl_3$.

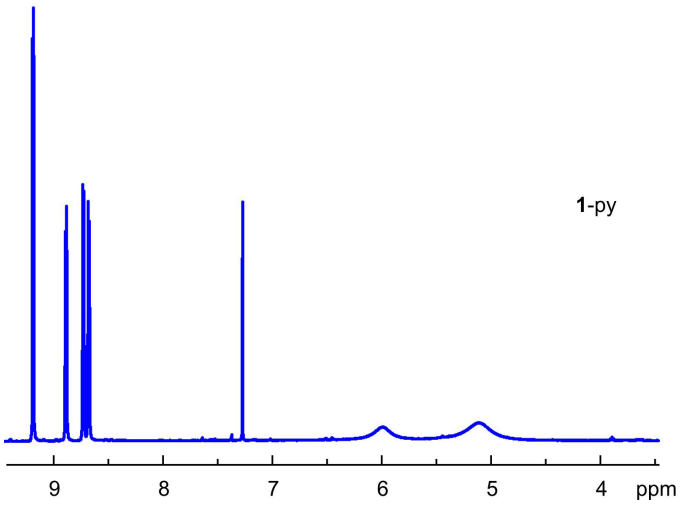

Figure S8. ^{1}H NMR spectrum of **1**-py in $CDCl_3$.

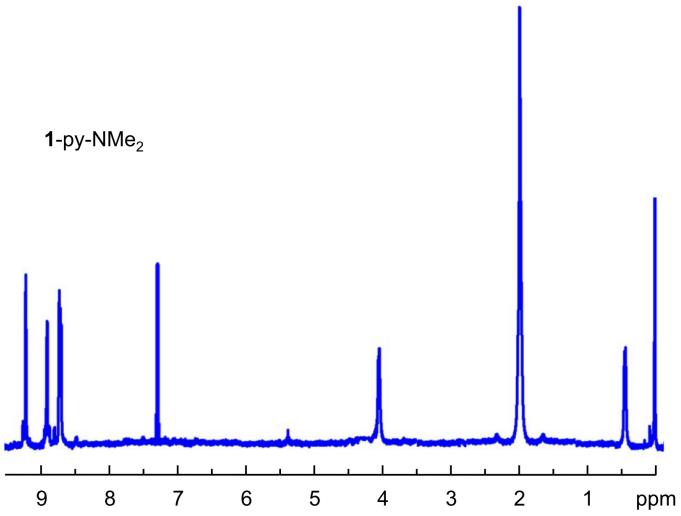

Figure S9. ^{1}H NMR spectrum of **1**-py-NMe_2 in $CDCl_3$.

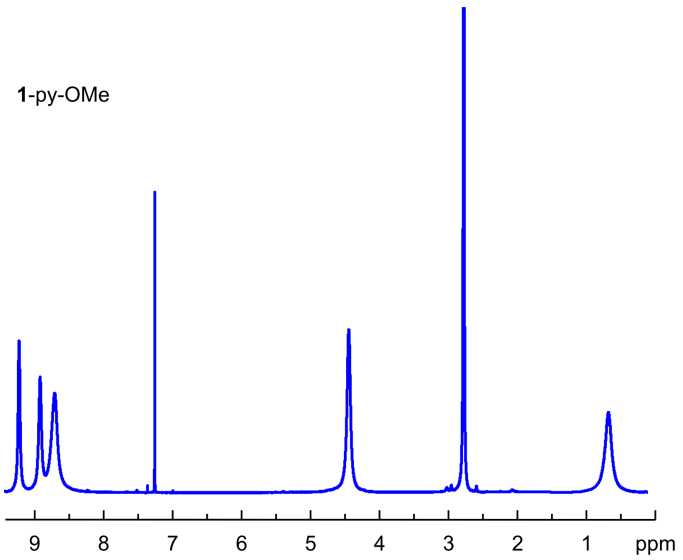

Figure S10. ^{1}H NMR spectrum of **1**-py-OMe in $CDCl_3$.

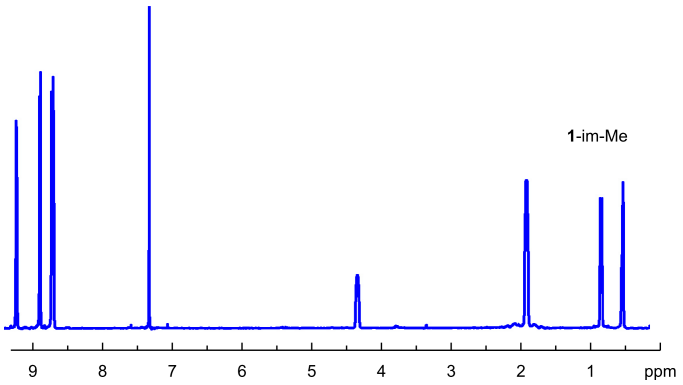

Figure S11. ^{1}H NMR spectrum of **1**-im-Me in $CDCl_3$.

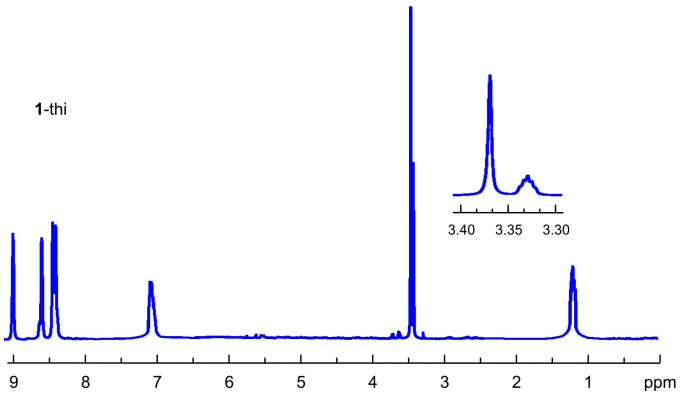

Figure S12. ^{1}H NMR spectrum of **1**-thi in CD_3OD.

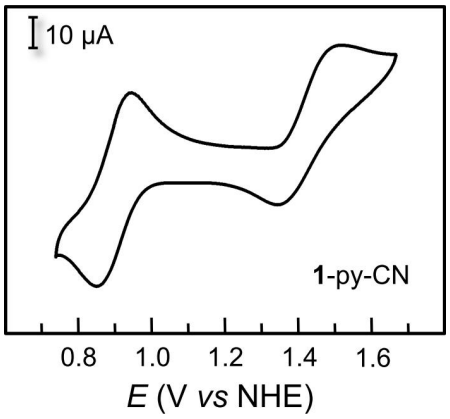

Figure S13. CV of **1**-py-CN (1.0 mM) in acetonitrile (0.1 M Bu_4NPF_6). Conditions: GC working electrode, Pt auxiliary electrode, Ag/Ag^+ reference electrode (calibrated using Fc^+/Fc), 50 mV s^{-1} scan rate.

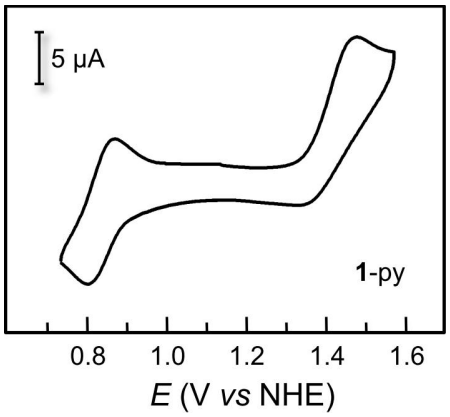

Figure S14. CV of **1**-py (1.0 mM) in acetonitrile (0.1 M Bu_4NPF_6). Conditions: GC working electrode, Pt auxiliary electrode, Ag/Ag^+ reference electrode (calibrated using Fc^+/Fc), 50 mV s^{-1} scan rate.

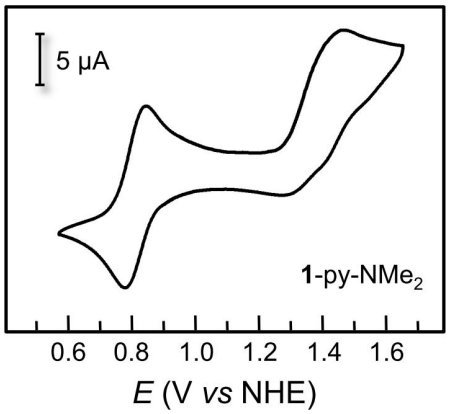

Figure S15. CV of **1**-py-NMe_2 (1.0 mM) in acetonitrile (0.1 M Bu_4NPF_6). Conditions: GC working electrode, Pt auxiliary electrode, Ag/Ag^+ reference electrode (calibrated using Fc^+/Fc), 50 mV s^{-1} scan rate.

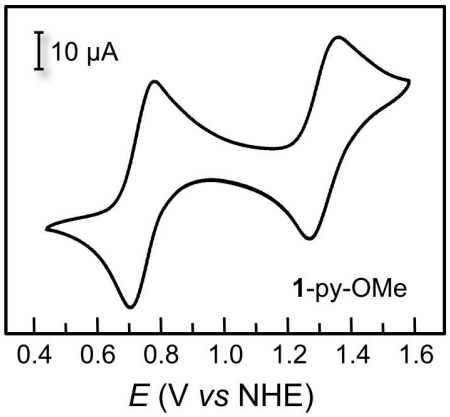

Figure S16. CV of **1**-py-OMe (1.0 mM) in acetonitrile (0.1 M Bu_4NPF_6). Conditions: GC working electrode, Pt auxiliary electrode, Ag/Ag^+ reference electrode (calibrated using Fc^+/Fc), 50 mV s^{-1} scan rate.

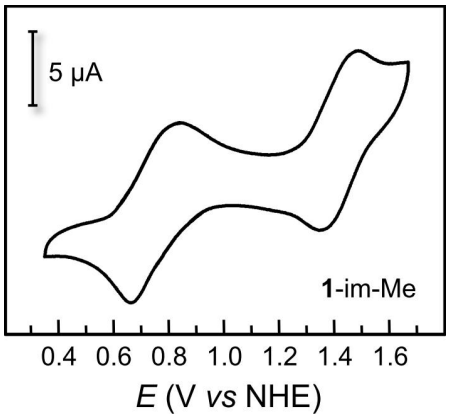

Figure S17. CV of **1**-im-Me (1.0 mM) in acetonitrile (0.1 M Bu_4NPF_6). Conditions: GC working electrode, Pt auxiliary electrode, Ag/Ag^+ reference electrode (calibrated using Fc^+/Fc), 50 mV s^{-1} scan rate.

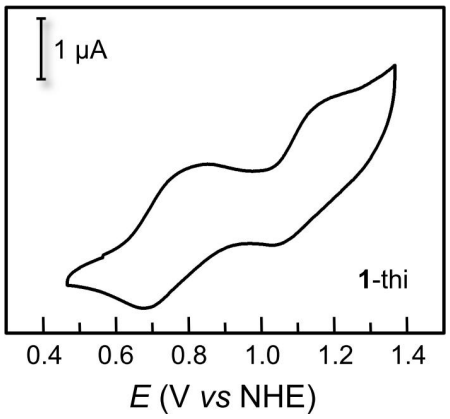

Figure S18. CV of **1**-thi (1.0 mM) in acetonitrile (0.1 M Bu_4NPF_6). Conditions: GC working electrode, Pt auxiliary electrode, Ag/Ag^+ reference electrode (calibrated using Fc^+/Fc), 50 mV s^{-1} scan rate.

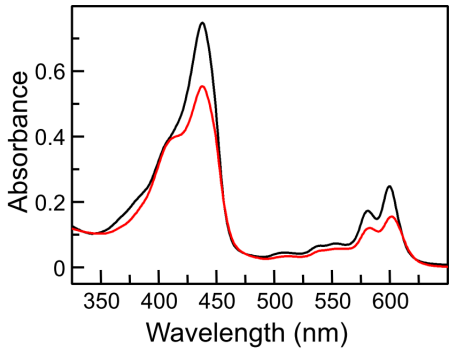

Figure S19. UV-vis spectra of **1**-py-OMe in acetonitrile before (black) and after (red) 20-h CPE at 1.0 V. Conditions: 0.1 M Bu_4NPF_6, GC working electrode, Pt auxiliary electrode, Ag/Ag^+ reference electrode, 20 °C.

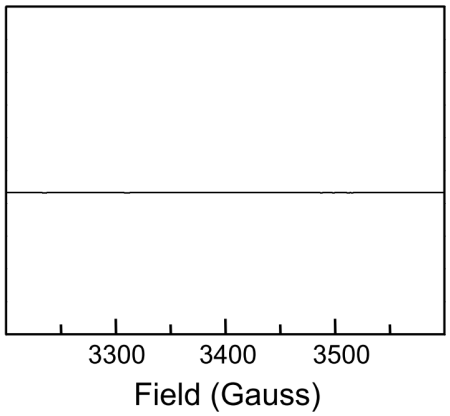

Figure S20. X-band EPR spectrum of **1**-py-OMe in acetonitrile at 90 K.

Table S1. Crystal data and structure refinement parameters for the X-ray structure of **1**-py-OMe.

Complex	**1**-py-OMe
molecular formula	$C_{49}H_{22}CoF_{15}N_6O_2$
formula wt. (g mol^{-1})	1070.66
temperature (K)	300(2)
radiation (λ, Å)	0.71073
crystal system	Monoclinic
space group	*C*2/c
a (Å)	30.225(3)
b (Å)	16.6117(11)
c (Å)	31.830(2)
β (°)	116.663(4)
Volume (Å^3)	14282.3(19)
Z	12
ρ_{calcd} (g cm^{-3})	1.494
μ (mm^{-1})	0.466
F(000)	6432
crystal size (mm^3)	0.20 × 0.20 × 0.20
Theta range	2.40 to 24.71°
reflections collected	202842
independent reflections	12113 [R(int) = 0.2010]
Completeness	99.4%
goodness-of-fit on F^2	1.089
final R indices	$R1^a$ = 0.0994
[R > 2σ (I)]	$wR_2{}^b$ = 0.2571
R indices (all data)	$R1^a$ = 0.1465
	$wR_2{}^b$ = 0.2980
largest diff. peak and hole (e Å^{-3})	1.738 and −0.485

$^a R_1 = \Sigma||F_o| - |F_c|| / |F_o|$, $^b wR_2 = \{\Sigma[w(F_o^2 - F_c^2)^2] / \Sigma[w(F_o^2)^2]\}^{0.5}$